

## **Heart Anatomy of *Rhincodon typus*: Three-dimensional X-ray Computed Tomography of Plastinated Specimens**

YUJI HIRASAKI<sup>1\*</sup>, TAKETERU TOMITA<sup>2</sup>, MAKIO YANAGISAWA<sup>2</sup>, KEIICHI UEDA<sup>2</sup>,  
KEIICHI SATO<sup>2</sup>, MASATAKA OKABE<sup>1</sup>

<sup>1</sup>Department of Anatomy, The Jikei University School of Medicine,  
3-25-8 Nishi-Shimbashi, Minato-ku, Tokyo, Japan

<sup>2</sup>Okinawa Churashima Research Center, Okinawa Churashima Foundation, 888 Ishikawa,  
Motobu-Cho, Okinawa, Japan

\*Correspondence to: Yuji Hirasaki, Department of Anatomy, The Jikei University School of  
Medicine, 3-25-8 Nishi-Shimbashi, Minato-ku, Tokyo, 105-8461, Japan

Phone: +81-3-3433-1111 Ext. 2206

Fax: +81-3-3433-2065

E-mail: [ug.hirasaki@gmail.com](mailto:ug.hirasaki@gmail.com)

Running title: Whale shark heart anatomy

Grant sponsor: The Jikei University Grant

## ABSTRACT

In the present study, we examined the structure of the heart of the whale shark, *Rhincodon typus*, using a plastination technique and three-dimensional X-ray computer tomography (3DCT). Inspection of the atrium revealed a symmetric distribution of the pectinate muscles attached to the commissures of the sino-atrial valve, suggesting some functional advantages. The majority of the ventricular wall comprised spongiosa, and compacta accounted for only ~3% of the entire thickness. There were three major fiber orientations in the spongiosa: the fibers on the endocardial side formed trabeculae that were aligned with the blood flow tract, whereas those on the epicardial side formed a circular pattern around the flow tract. Transluminal myofibers connected the inner and outer layers in the spongiosa, which may serve as an intraventricular conduction pathway.

Plastination and 3DCT is a powerful combination that allowed for multifaceted visualization of the internal structure of rare heart specimens in a non-destructive manner.

Key words: heart, myocardial architecture, plastination, X-ray computed tomography, whale shark.

## INTRODUCTION

The whale shark *Rhincodon typus* is the largest living fish in the world that inhabits tropical or warm oceans. While these fascinating fish have gained popularity among humans due to their large body size and placid nature, concerns have been raised regarding the sustainability of the species. In February 2016, the International Union for Conservation of Nature raised the Red List category of this species to “endangered” due to overexploitation. Several studies using satellite

tags have been performed to understand their ecology. These studies revealed that whale sharks travel long distances to pursue food or a warmer environment (Eckert and Stewart, 2001; Eckert et al., 2002; Hueter et al., 2013), and they are reported to dive to depths of approximately 1,900 m (Wilson et al., 2006; Tyminski et al., 2015). This gigantic fish may be endowed with special physical properties that enable them to travel across such a wide range of territories and depths.

The heart is a muscular organ that consistently pumps blood to the body against the workload. It is known that the architecture of the ventricular myocardium represents the activity of the given species. The elasmobranch heart ventricle possesses both inner spongiosa and outer compacta. Spongiosa is the major component of the ventricular wall in the elasmobranch, and compacta comprises no more than 40% of the ventricular wall (Santer and Greer Walker, 1980; Tota, 1983; Tota et al. 1983; Emery et al., 1985; Grimes and Kirby, 2009).

Scarce information is available on the structure of the whale shark heart. White (1936) first described the structure of the whale shark heart, but the major focus of that report was the conus arteriosus, and the morphology of other structures was not fully addressed.

Plastination is an organ preservation technique first developed by von Hagens (1979). In this technique, organic polymers are used to replace water and lipids in the tissue. Advantages of plastination over conventional preservation techniques include odorlessness, durability, and ease in handling (Riederer, 2014; Estai and Bunt, 2016). Despite its usefulness, inspection of the internal structures of the plastinated heart requires incision or resection of the tissue (Tiedemann and von Hagens, 1982; Gómez et al., 2012), which irreversibly changes the original shape of the organ. Changes made to the shape of rare specimens are a particularly serious issue.

In the present study, we assessed the morphology of plastinated whale shark heart specimens using three-dimensional X-ray computed tomography (3DCT), focusing on the myocardial architecture of the ventricle. We also examined the histology of the whale shark ventricle to

assess the composition of the ventricular myocardium.

## **MATERIALS AND METHODS**

### *Heart specimens*

Four heart specimens (#1-4) were collected following autopsy of whale sharks incidentally captured by fishermen between 2006 and 2007. The total length, body weight, and weight of the heart were recorded at autopsy, and RHW was calculated as follows:  $RHW (\%) = \text{heart weight (kg)} \times 100 / \text{body weight (kg)}$ .

### *Plastination*

Three plastinated heart specimens were created. The hearts were washed with water and fixed in 10% formalin for seven days at room temperature. Hydrostatic pressure was applied by occluding the openings of the branchial arteries to prevent shrinkage (Tiedeman and von Hagens, 1982). In specimen #2, the ventral side of the heart was incised to expose the conal valve. The specimens were then dehydrated by placing them in 100% acetone at -20°C for eight weeks. For the next four weeks, the acetone was replaced with silicone (Silicone S, NK Shoji Inc., Nago, Japan) containing curing material (Curing material A, NK Shoji Inc.). Silicone cross-linking was facilitated in a chamber containing vaporized curing material (Curing material C, NK Shoji Inc.) at room temperature over a period of two weeks.

### *X-ray CT imaging*

X-ray CT scanning was performed using commercially available equipment (SOMATOM Definition AS+, Siemens, Munich, Germany) according to the following protocol: tube voltage = 120 kV, scan time = 1 s, slice thickness = 0.6 mm. The acquired datasets were analyzed using dedicated computer software (Syngo CT VA46A, Siemens, Munich, Germany) based on volume-rendered 3D or 2D reconstructed images. Colors were applied semi-automatically by the

software according to the CT values of the regions. Dimensions of the chambers were measured along the estimated orthogonal axes of the fish body.

### *Histology*

A transverse ventricle specimen was obtained from the mid-ventral wall of specimen #4. The specimen was fixed with 10% formalin, dehydrated in ethanol, and then embedded in a paraffin block. The specimen was sectioned at 4- $\mu$ m thickness using a microtome. Microscopic assessment was performed using a digital microscope (BX53, Olympus, Tokyo, Japan) following hematoxylin-eosin staining.

## **RESULTS**

### *Overview of the heart specimens*

The profiles of the fish and heart specimens are summarized in Table 1. The heart weight and RHW was  $2.13 \pm 0.54$  kg (mean  $\pm$  SD) and  $0.17 \pm 0.02\%$ , respectively. All plastinated hearts contained the wall of the sinus venosus, atrium, ventricle, conus arteriosus, and the proximal end of the ventral aorta (Fig. 1,2). Specimen #3 contained the entire ventral aorta and sinus venosus. The dimensions of the atrium, ventricle, conus arteriosus, and atrioventricular valve for each specimen are summarized in Table 2.

### *Atrium and sinus venosus*

The atrium has a triangular shape and the largest volume among the four cardiac chambers. The atrium is located anterior to the sinus venosus, a thin-walled sac that collects venous blood from the duct of Cuvier and the hepatic veins. The sino-atrial (SA) valve, a large bileaflet valve, is interposed between the two chambers opening in the middle of the posterior atrial wall. Observation of the internal atrial wall revealed pectinate muscles lining most of the atrial wall,

many of which were attached to the commissures of the SA valve radiating in the antero-lateral direction (Fig. 3).

### *Ventricle*

The ventricle has an asymmetric shape, with its atrio-ventricular (AV) and cono-ventricular orifices aligned in a left-to-right configuration. A horizontal cut image of the reconstructed 3DCT dataset showed that a muscular ridge, namely a cono-ventricular fold (van Mierop and Kutsche, 1981) lying in the dorso-ventral direction between the two orifices, formed an arch that subdivided the ventricle into the ventricular inlet (left) and outlet (right, Fig. 4A, B). The ventricular inlet was connected to the atrium via the AV ring (Farrell and Jones, 1992), which contained the AV valve (Fig. 3A). The AV valve was bileaflet and attached to the ventricular wall either directly or via chords. In the axial cut image, the thickness of the ventricular wall was approximately 30 mm at the free wall, whereas it was thicker at the ventricular base (Fig. 4C). A high-density layer with a thickness of approximately 5 mm was seen along the epicardial as well as endocardial surfaces of the ventricle. The high-density layer was also seen on the cut surface of the spongiosa in specimen #2 (Fig. 4D) and therefore considered an artifact not representing the true nature of the original tissue. The internal aspect of the ventricle was significant for the presence of thick trabeculae. The trabeculae in the inlet were oriented dorso-ventrally, whereas those in the outlet were oriented antero-posteriorly. A convergence of trabeculae was observed at the apex. The middle layer demonstrated a complex meshwork of spongiosa surrounded by the lacunar system replaced by air. Manipulation of the data to make the high-density layers translucent revealed that the myofibers in the spongiosa formed a circular pattern around the atrioventricular valve, ventricular apex, and outlet (Fig. 5).

Myocardial architecture was further assessed using reconstructed 2D slice images, which revealed three major groups of myofibers with different fiber orientations in the spongiosa.

Namely, myofibers on the endocardial side (inner layer) were oriented in the same direction as the trabeculae and sent branch fibers across the ventricular wall toward the epicardium (transmural fibers). Sagittal slice images demonstrated that some trabeculae connected the atrioventricular junction and apex. The myofibers on the epicardial side (outer layer) formed clusters due to the insertion of the transmural fibers (Fig. 6). These findings were also seen in the cut surface of the ventricle in specimen #2 (Fig. 1D).

#### *Histology of the ventricle*

Histology of the ventricular myocardium revealed that the spongiosa occupied almost the entire ventricular wall. The compacta comprised a single layer and accounted for approximately 3% (1 mm) of the ventricular wall thickness. Compacta and spongiosa were differentiated by the “crisscrossed” fiber orientation (Brill and Chin Lai, 2015) and the presence of a lacunar system around the myocardial bundles in the spongiosa. Coronary vasculature was observed mainly in the epicardium and the transitional zone between the compacta and the spongiosa. However, it was also seen in the myocardial layer of both the compacta and spongiosa (Fig. 7).

#### *Conus arteriosus, ventral aorta, and coronary vessels*

The conus arteriosus consists of compact myocardium and two rows of thick tricuspid valves (Fig. 8A, B). The ventral aorta in specimen #3 was approximately 30 cm long and had four pairs of orifices of the afferent branchial arteries (Fig. 8C). It was confirmed at harvesting that the most distal orifice served as the common outlet for the first and second afferent branchial arteries. The orifice of the fifth branchial artery was located dorso-medially compared to the others.

A pair of coronary arteries descended along the antero-lateral surface of the conus arteriosus to distribute branch vessels on the ventricular surface (Fig. 8D). Superficial cardiac veins gathered around the AV ring to form a coronary sinus that opened at the left proximity to the SA valve in the sinus venosus (Fig. 8E, F).

## DISCUSSION

### *Methodology*

In the present study, the anatomy of the plastinated whale shark heart was assessed by 3DCT imaging. The large-scale heart specimens revealed interesting morphologic characteristics of the atrial and ventricular myocardium that have not been previously reported. Plastinated heart specimens are advantageous for acquiring CT datasets as they can stand alone. The presence of air functions as a negative contrast, allowing for high-quality imaging of the internal structures. Furthermore, digitalized image datasets allow for the removal of unnecessary parts of the heart in a non-destructive manner. The cut image of the ventricle demonstrated a homogeneous layer with a 5-mm surface thickness. This layer, resembling compacta, was considered an artifact of the formation of a silicone layer, since the layer was also observed on the cut surface of the spongiosa. Histologic confirmation was therefore necessary to directly measure the thickness of the compacta.

### *Gross morphology of the whale shark heart and relative heart weight*

The overall characteristics of the whale shark heart were similar to those of other elasmobranch fish (Parker, 1886; White, 1936; Santer and Greer Walker, 1980; van Mierop and Kutsche, 1981; Tota, 1999; Icardo, 2017). The RHW reflects the level of physical activity of the given species. Typically, a higher RHW is seen in physically active animals such as mammals and birds. Poupa and Lindström (1983) demonstrated that Selachii have a relatively high RHW for fish (0.196%). The RHW of the whale sharks in our study was within this range and therefore not specific.

### *Architecture of the atrium*

The internal architecture of the atrium was remarkable in the presence of pectinate muscles attaching to the SA valve. It has been shown that pacemaker cells are located adjacent to the SA valve in the vertebrate heart (Keith and Flack, 1907; Lange et al, 1966; van Mierop, 1967; Komuro et al, 1986; Haverinen and Vornanen, 2007; Tessadori et al, 2012). Furthermore, pectinate muscles in the chick embryo form the conduction pathway (Sedmera et al, 2006). It can therefore be speculated that pacemaker cells are located in the SA junction in the whale shark as well and that action potentials radiate via the pectinate muscles.

It is of note that the central location of the SA valve and the distribution pattern of the pectinate muscles make the overall morphology of the whale shark atrium somewhat symmetric. The symmetric distribution of pectinate muscles may be advantageous to synchronize the contraction of the atrial wall and to effectively transport the blood into the ventricle. The symmetric aspect of the single atrium stands in contrast to the two-chambered, asymmetric shape of the atrium in tetrapods, in which the SA valve is deviated to the right and the chamber divided by the atrial septum to the left of the SA valve. Our findings imply that the symmetry of the single atrium has been lost in tetrapods as a result of architectural changes associated with evolution.

#### *Myocardial architecture of the ventricle*

The fish heart ventricle is categorized into four types based on the presence of the coronary vasculature and the proportion of compacta. In general, elasmobranchs have a mixed-type ventricle that is categorized as either type III or IV, as the coronary system and compacta are always present (Tota, 1983; Grimes and Kirby, 2009). The compacta in type III ventricles accounts for less than 30% of the entire ventricle and is seen in sedentary or bottom-dwelling species. On the other hand, the type IV ventricle consists of compacta at a proportion greater than 30% and is seen in highly active endothermic sharks or tunas (Basile et al., 1976; Emery et

al., 1985; Sanchez-Quintana and Hurle, 1987). Our study revealed that despite its large body size, the whale shark has a type III ventricle with extremely thin compacta, accounting only for approximately 3% of the ventricular wall thickness. This percentage is similar to that in *Holocephali* (Durán et al., 2015). We consider that this finding corresponds to the nature of whale sharks as placid, slow swimmers. Furthermore, this finding implies that the whale sharks' horizontal and vertical movements in the ocean may not pose a significant workload on the ventricle.

The spongiosa comprised myofibers with different fiber orientations, which formed crisscrossed appearance in the cut images. In contrast to the general understanding of the architecture of the spongiosa being anarchic (Tota et al., 1983; Sanchez-Quintana et al., 1996), however, our study revealed layer-specific, flow-oriented fiber alignments in the whale shark ventricular spongiosa. Namely, the myofibers on the endocardial side (inner layer) were oriented along the ventricular flow tract, whereas those on the epicardial side (outer layer) form a circular pattern along the tract. There were also myofibers directed transmurally. It can be speculated that each group of fibers play a significant role not only in interventricular conduction but also in ventricular mechanics. The myofibers of the inner layer are considered responsible for the transmission of action potentials from the atrium through the flow tract. As seen in the *Xenopus* and zebrafish (Sedmera et al., 2003), the trabeculae in the ventricular inlet may contribute to the transmission of action potentials from the atrio-ventricular junction to the apex. Transmural fibers are believed to transmit action potentials to the outer layer. Contraction of the fibers in the outer layer is believed to constrict the flow tract. These fiber alignments are advantageous to efficiently generate an ejection force from the ventricular spongiosa. Further studies are necessary to elucidate whether the myocardial architecture seen in the present study is unique to the whale shark or if it also found in other elasmobranch fishes.

## **STUDY LIMITATIONS**

Our study has several limitations. First, the architecture of the ventricular compacta was compromised due to the presence of white epicardium and artifact formation, the latter presumably caused by silicone. The proportion of the compacta was assessed not based on the CT images but a histology specimen. Second, the proportion of the compacta was calculated based on the thickness. As significant methodological variability exists in literature for measuring the proportion of compacta, (Icardo, 2017), comparing the proportion of compacta among fish species requires caution. Third, the scarcity of specimens limited the extent of histological assessment on the whale shark heart in this study.

## **CONCLUSIONS**

The structure of the whale shark heart was assessed using 3DCT imaging, which allowed for visualization of the internal structure of rare heart specimens in a non-destructive manner. Our study revealed ordered myocardial fiber alignments in both the atrium and ventricle, suggesting some functional advantages. Histology revealed that the whale shark has a type III ventricle comprising an extremely thin compact myocardial layer, consistent with their placid nature.

## **ACKNOWLEDGMENTS**

We thank Naotsugu Shoji (plastination curator, NK Shoji Inc., Nago, Japan) for technical assistance in creating the plastinated heart specimens. We also thank all faculty members of

Department of Anatomy, The Jikei University School of Medicine for providing valuable insights and suggestions. This study was funded by the Jikei University Grant.

## LITERATURE CITED

- Basile C, Goldspink G, Modigh M, Tota B. 1976. Morphological and biochemical characterization of the inner and outer myocardial layers of adult tuna fish (*Thunnus thynnus* L.). *Comp Biochem Physiol B* 54:279-283.
- Brill R, Chin Lai N. 2015. Elasmobranch cardiovascular system. In: Shadwick, Farrell, Brauner, editors. *Physiology of elasmobranch fishes: Internal processes*. Fish Physiology. Vol. 34B. London: Academic Press. p 1-82.
- Durán AC, López-Unzu MA, Rodríguez C, Fernández B, Lorenzale M, Linares A, Salmerón F, Sans-Coma V. 2015. Structure and vascularization of the ventricular myocardium in Holocephali: their evolutionary significance. *J Anat* 226(6):501-510.
- Eckert SA, Stewart BS. 2001. Telemetry and satellite tracking of whale sharks, *Rhincodon typus*, in the Sea of Cortez, Mexico, and the North Pacific Ocean. *Environ Biol Fishes* 60:299-308.
- Eckert SA, Dolar LL, Kooyman GL, Perrin W, Rahman RA. 2002. Movements of whale sharks (*Rhincodon typus*) in Southeast Asian waters as determined by satellite telemetry. *J Zool* 257:111-115.
- Emery SH, Mangano C, Randazzo V. 1985. Ventricle morphology in pelagic elasmobranch fishes. *Comp Biochem Physiol* 82A:635-643.
- Estai M, Bunt S. 2016. Best teaching practices in anatomy education: a critical review. *Ann Anat* 208:151-157.
- Farrell AP, Jones DR. 1992. The heart. In: Hoar WS, Randall DJ, Farrell AP, editors. Part A: The Cardiovascular System. *Fish Physiology*. Vol. XII. New York: Academic Press. p 1-88.
- Gómez A, Del Palacio JF, Latorre R, Henry RW, Sarriá R, Albors OL. 2012. Plastinated heart slices aid echocardiographic interpretation in the dog. *Vet Radiol Ultrasound* 53:197-203.
- Grimes AC, Kirby ML. 2009. The outflow of the heart in fishes: anatomy, genes and evolution. *J Fish Biol* 74:983-1036.
- Haverinen J, Vornanen M. 2007. Temperature acclimation modifies sinoatrial pacemaker mechanism of the rainbow trout heart. *Am J Physiol Integr Comp Physiol* 292:R1023-R1032.
- Hueter RE, Tyminski JP, de la Parra R. 2013. Horizontal movements, migration patterns and

- population structure of whale sharks in the Gulf of Mexico and northwestern Caribbean Sea. *PLoS ONE* 6:1401-1416.
- Icardo JM. 2017. Heart morphology and anatomy. In: Gampel AK, Gillis TE, Farrel AP, Brauner CJ, editors. *The cardiovascular system: morphology, control and function. Fish Physiology. Vol. 36A.* Cambridge: Academic Press. p 1-54.
- Keith A, Flack M. 1907. The form and nature of the muscular connections between the primary divisions of the vertebrate heart. *J Anat Physiol* 41:172-189.
- Komuro H, Sakai T, Hirota A, Kamino K. 1986. Conduction pattern of excitation in the amphibian atrium assessed by multiple-site optical recording of action potentials. *Jpn J Physiol* 36:123-137.
- Lange G, Lu HH, Tsumuraya Y, Brooks CM. 1966. Pacemaker actions in the turtle heart. *Am J Physiol* 210(6):1375-1382.
- Parker TJ. 1886. On the blood-vessels of *Mustelus antarcticus*: a contribution to the morphology of the vascular system in the vertebrata. *Phil Trans R Soc Lond* 177:685-732.
- Poupa O, Lindsström L. 1983. Comparative and scaling aspects of heart and body weights with reference to blood supply of cardiac fibers. *Comp Biochem Physiol* 76A:413-421.
- Riederer BM. 2014. Plastination and its importance in teaching anatomy. Critical points for long-term preservation of human tissue. *J Anat* 224:309-315.
- Santer RM, Greer Walker M. 1980. Morphological studies on the ventricle of teleost and elasmobranch hearts. *J Zool Lond* 190:259-272.
- Sanchez-Quintana D, Hurle JM. 1987. Ventricular myocardial architecture in marine fishes. *Anat Rec* 217(3):263-273.
- Sanchez-Quintana D, García-Martínez V, Climent V, Hurlé JM. 1996. Myocardial fiber and connective tissue architecture in the fish heart ventricle. *J Exp Zool* 275:112-124.
- Sedmera D, Reckova M, De Almeida A, Sedmerova M, Biermann M, Volejnik J, Sarre A, Raddatz E, McCarthy RA, Gourdie RG, Thompson RP. 2003. *Am J Physiol Heart Circ Physiol* 284:H1152-H1160.
- Sedmera D, Wessels A, Trusk TC, Thompson RP, Hewett KW, Gourdie RG. 2006. Changes in activation sequence of embryonic chick atria correlate with developing myocardial architecture. *Am J Physiol Heart Circ Physiol* 291:H1646-H1652.
- Tessadori F, van Weerd JH, Burkhard SB, Verkerk AO, de Pater E, Boukens BJ, Vink A, Christoffels VM. 2012. Identification and functional characterization of cardiac pacemaker cells in zebrafish. *PLoS ONE* 7(10):e0047644.
- Tiedemann K, von Hagens G. 1982. The technique of heart plastination. *Anat Rec* 204:295-299.
- Tota B. 1983. Vascular and metabolic zonation in the ventricular myocardium of mammals and fishes. *Comp Biochem Physiol* 76A:423-37.

- Tota B, Cimini V, Salvatore G, Zummo G. 1983. Comparative study of the arterial and lacunary systems of the ventricular myocardium of elasmobranch and teleost fishes. *Am J Anat* 167:15-32.
- Tota B. 1999. Heart. In: Hamlett WC, editor. *Sharks, Skates, and Rays*. Baltimore: The John Hopkins Press. p 238-272.
- Tyminski JP, de la Parra-Venegas R, González Cano J, Hueter RE. 2015. Vertical movements and pattern in diving behavior of whale sharks as revealed by pop-up satellite tags in the eastern Gulf of Mexico. *PLoS ONE* 10:e0142156.
- van Mierop LH. 1967. Localization of pacemaker in chick embryo heart at the timing of initiation of heartbeat. *Am J Physiol* 212:407-415.
- van Mierop LH, Kutsche LM. 1981. Comparative anatomy of the ventricular septum. In: Wenink ACG, Oppenheimer-Dekker A, Moolaert AJ, editors. *The Ventricular Septum of the Heart*. Hague: Leiden University Press. p 35-46.
- von Hagens G. 1979. Impregnation of soft biological specimens with thermosetting resins and elastomers. *Anat Rec* 194:247-255.
- White EG. 1936. The heart valves of the elasmobranch fishes. *Am Mus Novit* 838:1-21.
- Wilson SG, Polovnia JJ, Stewart BS, Meekan MG. 2006. Movements of whale sharks (*Rhincodon typus*) tagged at Ningaloo Reef, Western Australia. *Mar Biol* 148:1157-1166.

#### Figure Legend

Figure 1. (A)-(C): External aspects of plastinated heart specimens #1 (A), #2 (B), and #3 (C). (D):

Sagittal cut surface of the ventral wall of specimen #2 showing crisscross appearance of the spongiosa. Asterisks indicate transluminal fibers.

An, anterior; At, atrium; CA, conus arteriosus; En, endocardium; Ep, epicardium; Po, posterior;

Sp, spongiosa; SV, sinus venosus; V, ventricle; VA, ventral aorta. Scale bars = 5 cm in (A-C) and 1 cm (D).

Figure 2. (A)-(E): Reconstructed three-dimensional images of the whale shark heart. Ventral (A), dorsal (B), left lateral (C), right lateral (D), and posterior (E) aspects of specimen #1. (F): Ventral aspect of specimen #2. (G): Left lateral aspect of specimen #3. For abbreviations, refer to Fig 1.

Scale bars = 5 cm.

Figure 3. (A)-(D): Structure of the atrium and sinus venosus of the whale shark.

Ventral (A), dorsal (B), lateral (C), and posterior (D) aspects of the internal atrial wall. Note the pectinate muscles attached at the commissures of the sino-atrial valve (asterisk) with symmetrical distribution. (E) and (F): The external (E) and internal (F) aspects of the sinus venosus showing openings of the duct of Cuvier (arrowheads) and hepatic veins (arrows). AVV, atrio-ventricular valve; SAV, sino-atrial valve. Scale bars = 5 cm.

Figure 4. (A) and (B): Horizontal cut images of the ventricle showing the dorsal (A) and ventral (B) aspects of the ventricular interior. Note the cono-ventricular fold (arrowheads) demarking the ventricular inlet (IL) and outlet (OL) and the different orientation of the trabeculae between the inlet and outlet. Majority of the ventricular wall comprises spongiosa with a complex meshwork. (C): Axial cut image of the ventricle. (D): Axial cut images of the ventricle in specimen #2 showing an artifact seen as a homogenous high-density layer on the cut surface of the spongiosa (asterisk). (E) and (F): Sagittal cut images of the ventricle showing the

atrio-ventricular connection (arrows) via atrio-ventricular valve (AVV). Scale bars = 5 cm.

Figure 5. (A)-(F): Ventral (A), dorsal (B), anterior (C), posterior (D), the left lateral (E), and right lateral (F) aspects of the ventricle showing the myocardial fiber orientation in the spongiosa. The data is adjusted so that the high-density layer on the ventricular surface appears translucent.

Note the myocardial fibers forming a circular pattern around the apex (asterisk, panel A), atrio-ventricular valve (AVV, B), and outlet (OL, C). Scale bars = 5 cm.

Figure 6. Reconstructed two-dimensional slice images of the ventricle. The signal intensity is affected by silicone and does not reflect the property of the original tissues. (A-C): Axial slice image of the conus arteriosus (CA, panel A) and outlet (B and C) demonstrating the circular arrangement of the myofibers. (D-G): Myofibers in the inner layer aligned along the inlet (asterisk) and transluminal fibers (arrowheads). Arrows indicate the atrio-ventricular connections. (H): Myofibers in the outer layer aligned perpendicularly to those in the inner layer. (I and J): Horizontal slice images demonstrating the circular arrangement of myofibers around the atrio-ventricular valve. (K and L): Sagittal slice images demonstrating trabeculae connecting the atrio-ventricular junction and apex. Scale bars = 5 cm.

Figure 7. Photomicrograph of the ventricular myocardium of the whale shark. (A): Montage photomicrograph of the ventricular wall to capture its entire thickness. Note that the majority of the ventricular wall consisted of spongiosa (Sp). (B): Enlarged image of the box in panel A showing the crisscrossed alignment of the myofibers. The thickness of the compacta (Co) is 1 mm, accounting for 3% of the entire thickness. Scale bar = 1 mm. (C): Enlarged image of the upper box in panel B showing the coronary artery in the Sp (arrow). (D): Enlarged image of the lower box in panel B showing the coronary vasculatures seen in the epicardium (Ep) and the transitional zone between the compacta and the spongiosa. A small vessel is also seen within the compacta (asterisk). Scale bars = 2 mm (A), 1 mm (B-D).

Figure 8. The structure of the conus arteriosus, ventral aorta, and coronary vessels. (A): Short axis view of the conal valve. Note the cross section of the coronary arteries (arrows). (B): Internal aspect of the conus arteriosus demonstrating two rows of conal valves. (C): Dorsal aspect of the ventral aorta showing four orifices of branchial arteries (I-V). Note that the most distal orifice serves as the common outlet for the first and second afferent branchial arteries (I + II). (D): Lateral aspect of the heart showing the coronary artery (arrow) and veins (arrowheads). (E): Coronary veins forming the sinus (arrowheads) around the atrio-ventricular ring. (F): The opening of the coronary sinus (asterisk) located in left-proximity to the sino-atrial valve (SAV) in

the sinus venosus (SV). Scale bars = 5 cm.

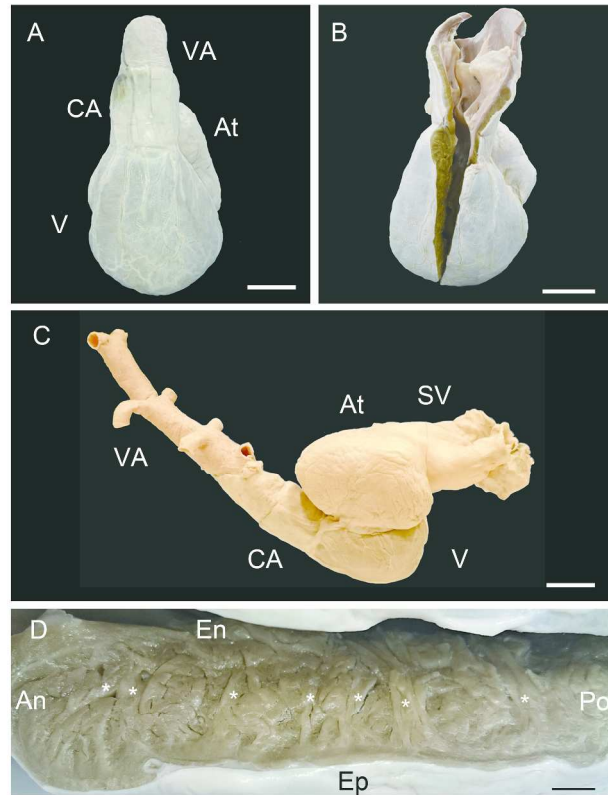
Table 1. Profiles of the individual whale shark, *Rhincodon typus*.

#	Sex	Total length (cm)	Body weight (kg)	Heart weight (kg)	Relative heart weight (%)
1	M	595	1050	2.05	0.195
2	F	665	1720	2.75	0.160
3	M	585	1260	2.25	0.179
4	M	573	965	1.45	0.150
Mean $\pm$ S.D.		605 $\pm$ 41	1249 $\pm$ 338	2.13 $\pm$ 0.54	0.171 $\pm$ 0.020

Table 2. The dimensions of the plastinated hearts.

#	Atrium (cm)	Ventricle (cm)	Ventricular wall thickness (mm)	Conus arteriosus (cm)	Atrio-ventricular valve (cm)
1	18.7 x 17.7 x 8.4	15.3 x 15.2 x 13.4	24.0	7.0x 7.0 x 7.0	5.4 x 5.7
2	14.2 x 16.3 x 11.0	N.A	27.7	N.A.	4.1 x 5.4
3	17.8 x 18.2 x 9.9	13.8 x 12.7 x 9.4	29.4	7.8 x 7.4 x 7.2	5.1 x 6.0

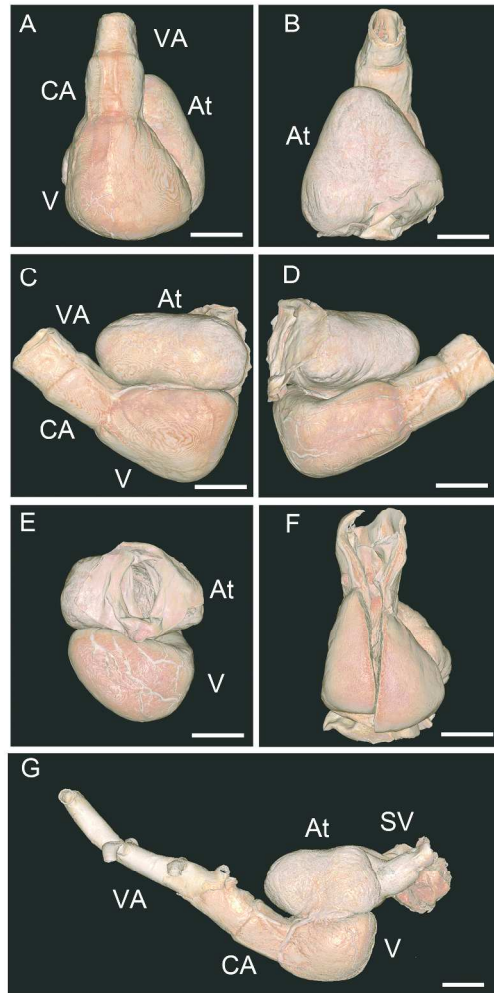
Dimensions are demonstrated as length x width x thickness. N.A.: not applicable.



(A)-(C): External aspects of plastinated heart specimens #1 (A), #2 (B), and #3 (C). (D): Sagittal cut surface of the ventral wall of specimen #2 showing crisscross appearance of the spongiosa. Asterisks indicate transluminal fibers.

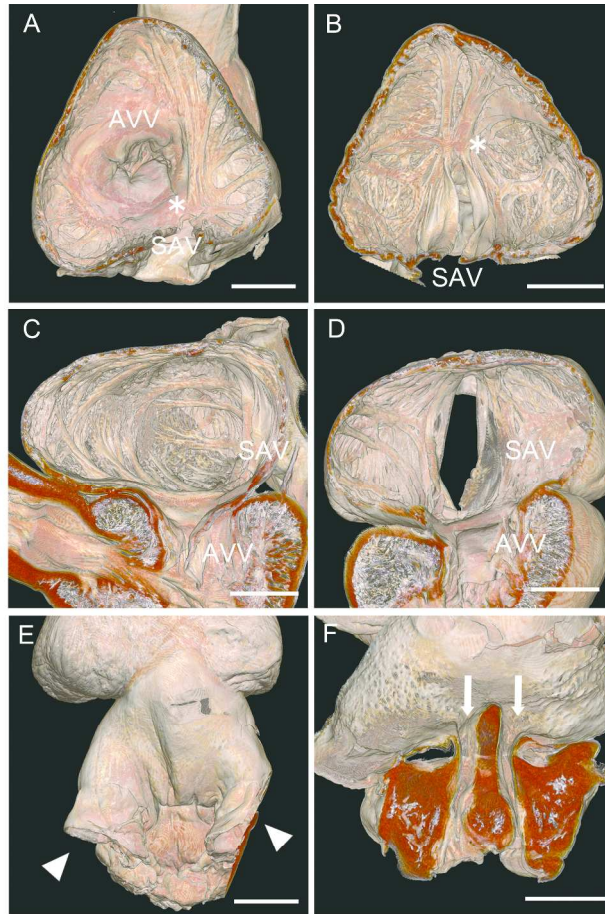
An, anterior; At, atrium; CA, conus arteriosus; En, endocardium; Ep, epicardium; Po, posterior; Sp, spongiosa; SV, sinus venosus; V, ventricle; VA, ventral aorta. Scale bars = 5 cm in (A-C) and 1 cm (D).

297x420mm (300 x 300 DPI)



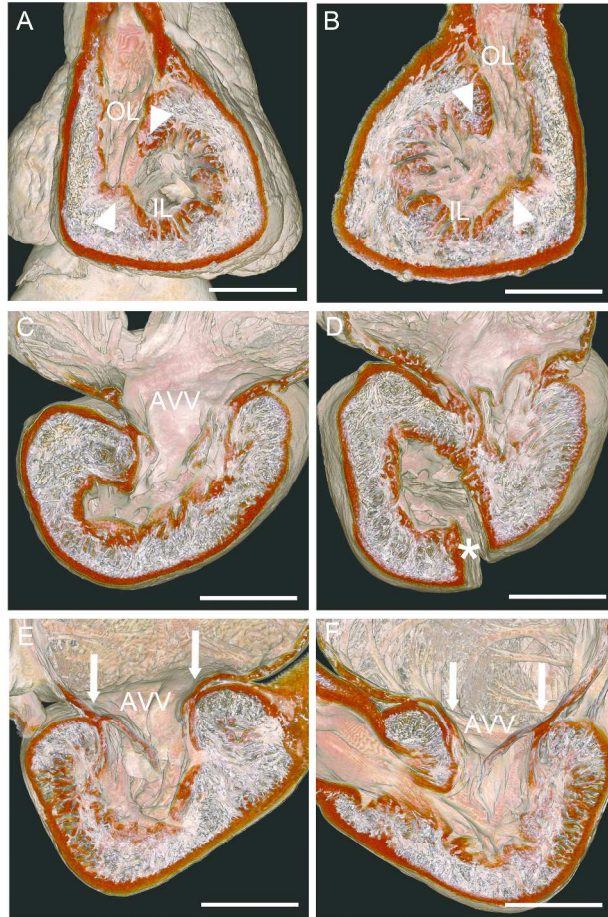
(A)-(E): Reconstructed three-dimensional images of the whale shark heart. Ventral (A), dorsal (B), left lateral (C), right lateral (D), and posterior (E) aspects of specimen #1. (F): Ventral aspect of specimen #2. (G): Left lateral aspect of specimen #3. For abbreviations, refer to Fig 1. Scale bars = 5 cm.

297x420mm (300 x 300 DPI)



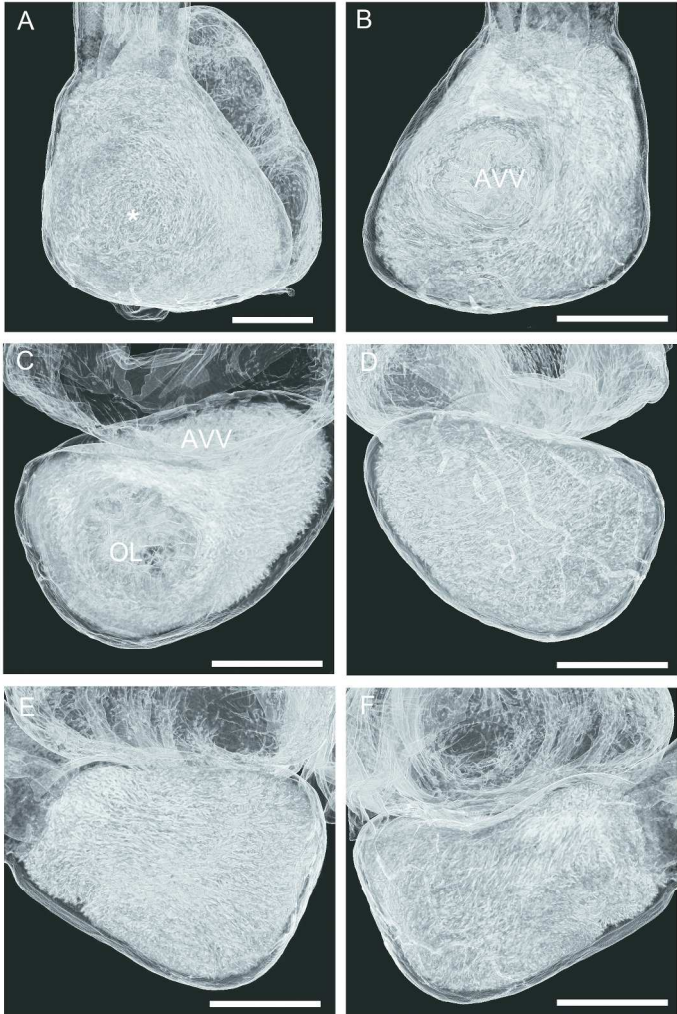
(A)-(D): Structure of the atrium and sinus venosus of the whale shark. Ventral (A), dorsal (B), lateral (C), and posterior (D) aspects of the internal atrial wall. Note the pectinate muscles attached at the commissures of the sino-atrial valve (asterisk) with symmetrical distribution. (E) and (F): The external (E) and internal (F) aspects of the sinus venosus showing openings of the duct of Cuvier (arrowheads) and hepatic veins (arrows). AVV, atrio-ventricular valve; SAV, sino-atrial valve. Scale bars = 5 cm.

297x420mm (300 x 300 DPI)



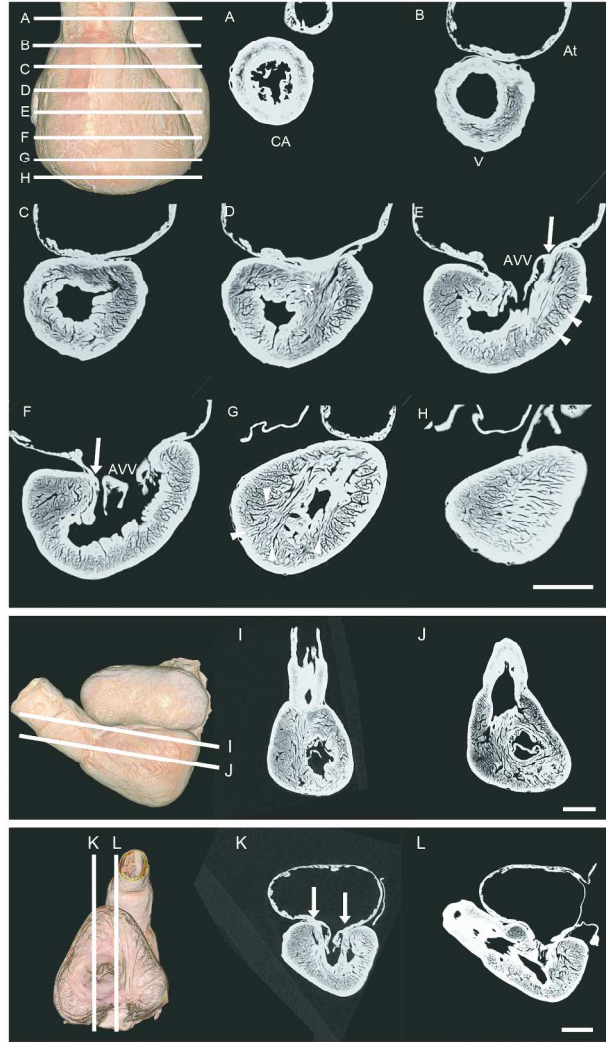
(A) and (B): Horizontal cut images of the ventricle showing the dorsal (A) and ventral (B) aspects of the ventricular interior. Note the cono-ventricular fold (arrowheads) demarcating the ventricular inlet (IL) and outlet (OL) and the different orientation of the trabeculae between the inlet and outlet. Majority of the ventricular wall comprises spongiosa with a complex meshwork. (C): Axial cut image of the ventricle. (D): Axial cut images of the ventricle in specimen #2 showing an artifact seen as a homogenous high-density layer on the cut surface of the spongiosa (asterisk). (E) and (F): Sagittal cut images of the ventricle showing the atrio-ventricular connection (arrows) via atrio-ventricular valve (AVV). Scale bars = 5 cm.

297x420mm (300 x 300 DPI)



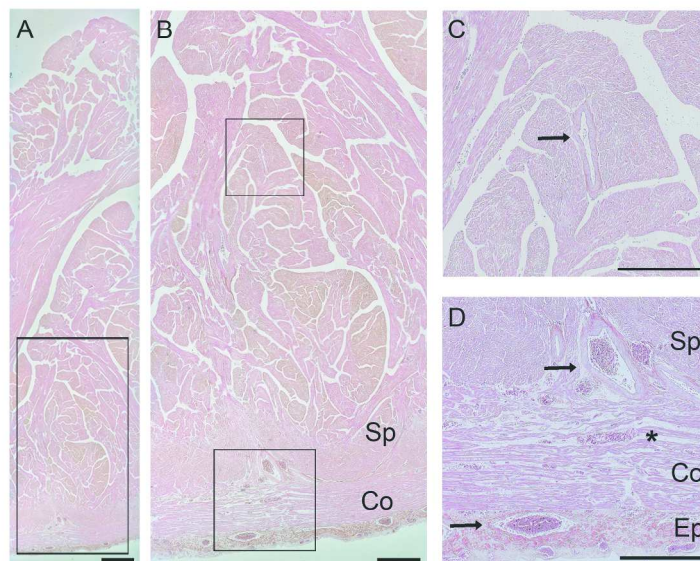
(A)-(F): Ventral (A), dorsal (B), anterior (C), posterior (D), the left lateral (E), and right lateral (F) aspects of the ventricle showing the myocardial fiber orientation in the spongiosa. The data is adjusted so that the high-density layer on the ventricular surface appears translucent. Note the myocardial fibers forming a circular pattern around the apex (asterisk, panel A), atrio-ventricular valve (AVV, B), and outlet (OL, C). Scale bars = 5 cm.

297x420mm (300 x 300 DPI)



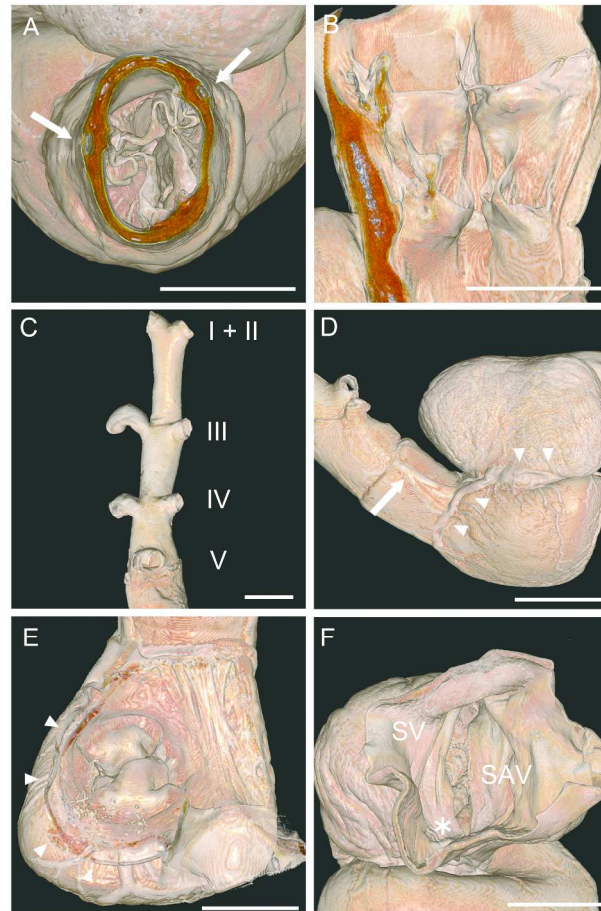
Reconstructed two-dimensional slice images of the ventricle. The signal intensity is affected by silicone and does not reflect the property of the original tissues. (A-C): Axial slice image of the conus arteriosus (CA, panel A) and outlet (B and C) demonstrating the circular arrangement of the myofibers. (D-G): Myofibers in the inner layer aligned along the inlet (asterisk) and transmural fibers (arrowheads). Arrows indicate the atrio-ventricular connections. (H): Myofibers in the outer layer aligned perpendicularly to those in the inner layer. (I and J): Horizontal slice images demonstrating the circular arrangement of myofibers around the atrio-ventricular valve. (K and L): Sagittal slice images demonstrating trabeculae connecting the atrio-ventricular junction and apex. Scale bars = 5 cm.

297x420mm (300 x 300 DPI)



Photomicrograph of the ventricular myocardium of the whale shark. (A): Montage photomicrograph of the ventricular wall to capture its entire thickness. Note that the majority of the ventricular wall consisted of spongiosa (Sp). (B): Enlarged image of the box in panel A showing the crisscrossed alignment of the myofibers. The thickness of the compacta (Co) is 1 mm, accounting for 3% of the entire thickness. Scale bar = 1 mm. (C): Enlarged image of the upper box in panel B showing the coronary artery in the Sp (arrow). (D): Enlarged image of the lower box in panel B showing the coronary vasculatures seen in the epicardium (Ep) and the transitional zone between the compacta and the spongiosa. A small vessel is also seen within the compacta (asterisk). Scale bars = 2 mm (A), 1 mm (B-D).

297x420mm (300 x 300 DPI)



The structure of the conus arteriosus, ventral aorta, and coronary vessels. (A): Short axis view of the conal valve. Note the cross section of the coronary arteries (arrows). (B): Internal aspect of the conus arteriosus demonstrating two rows of conal valves. (C): Dorsal aspect of the ventral aorta showing four orifices of branchial arteries (I-V). Note that the most distal orifice serves as the common outlet for the first and second afferent branchial arteries (I + II). (D): Lateral aspect of the heart showing the coronary artery (arrow) and veins (arrowheads). (E): Coronary veins forming the sinus (arrowheads) around the atrio-ventricular ring. (F): The opening of the coronary sinus (asterisk) located in left-proximity to the sino-atrial valve (SAV) in the sinus venosus (SV). Scale bars = 5 cm.

297x420mm (300 x 300 DPI)



This is an image file for consideration as a possible cover illustration of reconstructed three-dimensional computed tomographic images of the whale shark heart showing the dorsal (left) and ventral aspects of the atrial interior.

260x321mm (300 x 300 DPI)